

Thermoelectric property tailoring by composite engineering

V. H. GUERRERO, SHOUKAI WANG, SIHAI WEN, D. D. L. CHUNG
Composite Materials Research Laboratory, University at Buffalo, The State University of New York, Buffalo, NY 14260-4400, USA

The tailoring of the thermoelectric properties (the sign and magnitude of the absolute thermoelectric power) was achieved by composite engineering. The techniques involved the choice of the reinforcing fibers (continuous or short) in a structural composite and the choice of the particulate filler between the laminae in a continuous fiber composite. The tailoring resulted in thermoelectric structural composites, including continuous carbon fiber polymer-matrix composites and short fiber cement-matrix composites. In addition, it resulted in thermocouples in the form of structural composites. The choice of fibers impacted the thermoelectric behavior in the fiber direction of the composite. The choice of interlaminar filler impacted the thermoelectric behavior in the through-thickness direction.

© 2002 Kluwer Academic Publishers

1. Introduction

Composite engineering has been widely employed to tailor the strength, modulus, thermal expansion coefficient, electrical resistivity and thermal conductivity of materials. However, it has been little used for tailoring the thermoelectric properties, which are important for electrical energy generation, heating and cooling. Electrical energy generation involves the Seebeck effect, in which a temperature gradient gives rise to a voltage between the hot and cold ends. Heating and cooling involve the Peltier effect, in which heat is evolved (i.e., heating) or absorbed (i.e., cooling) upon passage of an electric current across two dissimilar materials that are electrically connected. The Seebeck effect provides a renewable source of energy, in addition to providing the basis for thermocouples, which are used for temperature measurement. Moreover, it is relevant to the reduction of environmental pollution and global warming. The Peltier effect is relevant to air conditioning, refrigeration and thermal management.

The tailoring of the Seebeck effect involves consideration of mainly a single property, namely the thermoelectric power. On the other hand, the tailoring of the Peltier effect requires consideration of three properties, namely the thermoelectric power, electrical resistivity and thermal conductivity. Composite engineering is valuable for tailoring both Seebeck and Peltier effects, although this paper is focused on the Seebeck effect.

Composite engineering involves artificial combination of different components, such as carbon fibers and a polymer matrix. It is to be distinguished from alloying, which involves diffusion and/or reaction that results in phases governed by thermodynamics. Although the different components of a composite can undergo diffusion or reaction at their interface, the diffusion or reaction is limited in spatial extent and the components

largely retain their original compositions during composite fabrication. On the other hand, composite engineering provides numerous parameters that facilitate tailoring of the properties. These parameters include the components (e.g., the matrix and the fillers), the continuity of the components (e.g., the fibrous filler being continuous or discontinuous), the orientation of the components (e.g., the fiber orientation), the relative orientation of the units of a component (e.g., continuous fibers being unidirectional or crossply), the volume fractions of the components, the degree of contact among the units of a component (e.g., the degree of contact among particles of a particulate filler and among the fibers of a fibrous filler), the interface between components (e.g., the fiber-matrix interface), the interface between units of a component (e.g., the interface between laminae in a laminate), etc.

Because fibers are effective as a reinforcement, fibrous composites tend to exhibit good mechanical properties, particularly when the fibers are continuous. Therefore, fibrous composites have been developed for structural applications. The most common structural composites are polymer-matrix composites containing continuous fibers, as used for lightweight structures such as aircraft, sporting goods and machinery. Increasingly common are cement-matrix composites containing short fibers, as used in construction due to their low drying shrinkage and enhanced flexural toughness. Continuous fibers are not common for cement-matrix composites due to their high cost and the requirement of low cost for a practical concrete.

The approach used in this work involves taking structural composites as a starting point and modifying these composites for the purpose of enhancing the thermoelectric properties. In this way, the resulting composites are multifunctional (i.e., both structural

and thermoelectric). Because structural composites are used in large volumes, the rendering of the thermoelectric function to these materials means the availability of large volumes of thermoelectric materials for use in, say, electrical energy generation. Moreover, temperature sensing is useful for structures for the purpose of thermal control, energy saving and hazard mitigation. The rendering of the thermoelectric function to a structural material also means that the structure can sense its own temperature without the need for embedded or attached thermometric devices, which suffer from high cost and poor durability. Embedded devices, in particular, cause degradation of the mechanical properties of the structure.

The paper addresses the tailoring of the thermoelectric properties of structural composites, specifically cement-matrix composites containing short and randomly oriented fibers, and polymer-matrix composites containing continuous and oriented fibers. In both cases, the fibers serve as the reinforcement.

Two routes are used in the tailoring. One route involves the choice of fibers. The other route, which only applies to the polymer-matrix composites, involves the choice of the interlaminar filler, which refers to the particulate filler between the laminae. The former route impacts the thermoelectric properties in any direction for a composite containing randomly oriented fibers. In the case of a composite containing oriented continuous fibers, the former route impacts mainly the thermoelectric properties in the fiber direction of the composite, whereas the latter route impacts mainly the thermoelectric properties in the through-thickness direction of the composite.

2. Tailoring by the choice of fibers

2.1. Polymer-matrix composites

Polymer-matrix composites with continuous oriented carbon fibers are widely used for aircraft, sporting goods and other lightweight structures. Glass fibers and polymer fibers are less expensive than carbon fibers, but they are not conductive electrically and are therefore not suitable for rendering the thermoelectric function to the composite.

Graphite is a semi-metal. Due to charge transfer between carbon and the intercalate, intercalation by an electron donor makes it an electron metal, whereas intercalation by an electron acceptor makes it a hole metal [1–3]. Carbon fibers differ from graphite in that they are not completely crystalline. They can be slightly n-type or slightly p-type, depending on their grade, even without intercalation. Intercalation greatly increases the carrier concentration, thus making the fibers strongly n-type or p-type, depending on whether the intercalate is an electron donor or an electron acceptor [4].

One of the drawbacks of intercalated graphite is the instability over time, either due to intercalate desorption or reaction with environmental species. For the case of bromine (acceptor) as the intercalate, the instability due to desorption can be overcome by the use of a residue compound, i.e., a compound that has undergone desorption as much as possible so that the remaining intercalate is strongly held, thereby making the

compound stable. The stability of bromine intercalated carbon fibers has been previously demonstrated [5–7]. For the case of an alkali metal such as sodium (donor) as the intercalate, the instability due to reactivity with moisture can be overcome by the use of an alkali metal hydroxide (with the alkali metal ions in excess) as the intercalate [8]. Therefore, this paper uses bromine as the acceptor intercalate and sodium hydroxide (with Na^+ ions in excess) as the donor intercalate.

Although considerable attention has been given to intercalated carbon fibers, little attention has been given to composites that involve these fibers [9–11]. Previous work on these composites has been focused on the electrical conductivity, due to the relevance to electromagnetic interference shielding and other applications.

The carbon fibers used were Thornel P-25, P-100 and P-120 2K pitch-based fibers (Amoco Performance Products, Alpharetta, GA) and T-300 PAN-based fibers (in the form of 976 epoxy unidirectional fiber preregs, Hy-E 1076E, ICI Fiberite, Tempe, AZ). The degree of crystallinity of the Thornel series of carbon fibers increases in the order: P-25, P-100 and P-120. The PAN-based carbon fiber tend to be weak in crystallinity [12].

Intercalation was carried out only for P-100 and P-120 fibers, due to their relatively high crystallinity. Bromine intercalation involved exposure to bromine vapor in air at room temperature for 10 days, followed by desorption in a fume hood at room temperature for several months [13]. Sodium hydroxide intercalation involved immersion of the fibers in a liquid solution of NaOH and molten sodium contained in a nickel crucible [8]. The atomic ratio of Na to NaOH was 1:100. The procedure is described below. The crucible was placed in a small furnace, which was purged with argon gas. After the furnace had reached 350°C , sodium metal was added to the molten NaOH in the crucible. Then the fibers (protected by a nickel spring) were immersed in the liquid solution. The furnace was covered and the temperature of 350°C was maintained for 4 h. After that, the fibers were removed and allowed to cool. Then the fibers (still protected by a nickel spring) were washed by flowing water for 12 h in order to remove the NaOH on the fiber surface. After this, the fibers were dried in a vacuum oven. The intercalate concentrations in the fibers were not determined, but they are expected to be low compared to the saturation values, due to the extensive desorption that occurred after intercalation.

Thermocouple junctions were epoxy-matrix composite interlaminar interfaces. In this study, a junction was formed by allowing two laminae to overlap partially and then curing the stack under heat and pressure, as required for the curing of the epoxy matrix. The overlap region served as the junction; the remaining regions served as thermocouple wires. Those junctions involving T-300 fibers used the epoxy in the prepreg as the bonding agent for the junction. Those not involving T-300 fibers used epoxy resin 9405 and curing agent 9470 from Shell Chemical Co. (Houston, TX) as the epoxy matrix as well as bonding agent. Curing of the epoxy in the T-300 prepreg was conducted by heating in a hydraulic hot press at a rate of $2.5^\circ\text{C}/\text{min}$ and then maintaining the temperature for 2 h. The curing

temperature was 175°C for the epoxy in the T-300 prepregs and was 150°C for the other epoxy. The curing pressure was 18 MPa for unidirectional junctions (i.e., the fibers in the two laminae oriented in the same direction) and 16 MPa for crossply junctions (i.e., the fibers in the two laminae oriented at 90°) involving the epoxy in the T-300 prepregs. For junctions involving the other epoxy, the curing pressure was 0.02 MPa.

Thermopower measurement was performed on the fibers (P-25, P-100 and P-120 fiber bundles without matrix, and T-300 prepreg with epoxy matrix) and on the epoxy-matrix composite junctions involving dissimilar fibers. The measurement in the former case involved attaching the two ends of a fiber bundle or prepreg to copper foils using a silver-epoxy conducting adhesive, maintaining one copper foil at a controlled high temperature (up to 200°C) by using a furnace, and maintaining the other copper foil at a temperature near room temperature. A copper wire was soldered at its end to each of the two copper foils. The copper wires were fed to a Keithley 2001 multimeter for measuring the voltage. T-type thermocouples were used for measuring the temperatures of the hot and cold ends. Voltage and temperature measurements were done simultaneously using the multimeter. The voltage difference (hot minus cold) divided by the temperature difference (hot minus cold) yielded the Seebeck coefficient with copper as the reference, since the copper wires at the two ends of a sample were at different temperatures. This Seebeck coefficient minus the absolute thermoelectric power of copper (+2.34 $\mu\text{V}/^\circ\text{C}$) [14] is the absolute thermoelectric power of the composite. The thermopower measurement in the latter case involved the same configuration, except that the junction was at the hot point and the two ends of the sample away from the junction were attached using silver-epoxy onto two copper foils, which were both at a temperature near room temperature.

Table I shows the Seebeck coefficient and the absolute thermoelectric power of composites and the ther-

TABLE I Seebeck coefficient ($\mu\text{V}/^\circ\text{C}$) and absolute thermoelectric power ($\mu\text{V}/^\circ\text{C}$) of carbon fibers and thermocouple sensitivity ($\mu\text{V}/^\circ\text{C}$) of epoxy-matrix composite junctions. All junctions are unidirectional unless specified as crossply. The temperature range is 20–110°C

	Seebeck coefficient with copper as the reference ($\mu\text{V}/^\circ\text{C}$)	Absolute thermoelectric power ($\mu\text{V}/^\circ\text{C}$)	Thermocouple sensitivity ($\mu\text{V}/^\circ\text{C}$)
P-25 ^a	+0.8	-1.5	
T-300 ^a	-5.0	-7.3	
P-25 ^a + T-300 ^a			+5.5
P-25 ^a + T-300 ^a (crossply)			+5.4
P-100 ^a	-1.7	-4.0	
P-120 ^a	-3.2	-5.5	
P-100 (Na)	-48	-50	
P-100 (Br ₂)	+43	+41	
P-100 (Br ₂) + P-100 (Na)			+82
P-120 (Na)	-42	-44	
P-120 (Br ₂)	+38	+36	
P-120 (Br ₂) + P-120 (Na)			+74

^aPristine (i.e., not intercalated).

mocouple sensitivity of composite junctions. A positive value of the absolute thermoelectric power indicates p-type behavior; a negative value indicates n-type behavior. Pristine P-25 is slightly n-type; pristine T-300 is strongly n-type. A junction comprising pristine P-25 and pristine T-300 has a positive thermocouple sensitivity that is close to the difference of the Seebeck coefficients (or the absolute thermoelectric powers) of T-300 and P-25, whether the junction is unidirectional or crossply. Pristine P-100 and pristine P-120 are both slightly n-type. Intercalation with sodium causes P-100 and P-120 to become strongly n-type. Intercalation with bromine causes P-100 and P-120 to become strongly p-type. A junction comprising bromine intercalated P-100 and sodium intercalated P-100 has a positive thermocouple sensitivity that is close to the sum of the magnitudes of the absolute thermoelectric powers of the bromine intercalated P-100 and the sodium intercalated P-100. Similarly, a junction comprising bromine intercalated P-120 and sodium intercalated P-120 has a positive thermocouple sensitivity that is close to the sum of the magnitudes of the absolute thermoelectric powers of the bromine intercalated P-120 and the sodium intercalated P-120. Fig. 1 shows the linear relationship of the measured voltage with the temperature difference between hot and cold points for the junction comprising bromine intercalated P-100 and sodium intercalated P-100. By using junctions comprising strongly n-type and strongly p-type partners, a thermocouple sensitivity as high as +82 $\mu\text{V}/^\circ\text{C}$ was attained.

It is important to note that the thermocouple junctions do not require any bonding agent other than the epoxy, which serves as the matrix of the composite and does not serve as an electrical contact medium (since it is not conducting). In spite of the presence of the epoxy matrix in the junction area, direct contact occurs between a fraction of the fibers of a lamina and a fraction of the fibers of the other lamina, thus resulting in a conduction path in the direction perpendicular to the junction. This conduction path is indicated by direct measurement of the electrical resistance of the junction [15] and enables an electrical contact to be made across the junction. The use of silver paint as an additional bonding agent

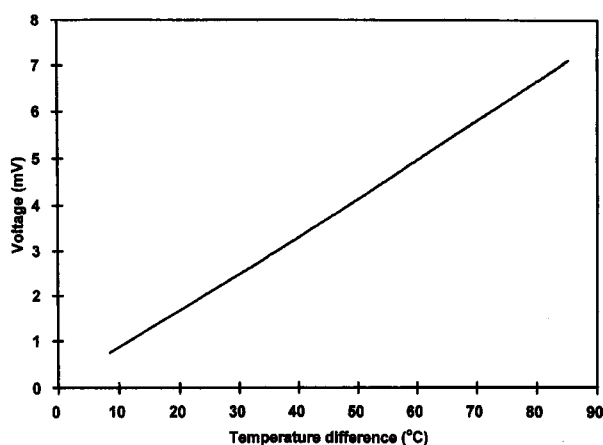


Figure 1 Variation of the measured voltage with the temperature difference between hot and cold points for the epoxy-matrix composite junction comprising bromine intercalated P-100 and sodium intercalated P-100.

did not give better result, as we found experimentally. That a bonding agent did not affect the result is also consistent with the fact that the thermocouple effect is not an interfacial phenomenon. That an additional bonding agent is not necessary facilitates the use of a structural composite as a thermocouple array, as a typical structural composite does not have any extra bonding agent at the interlaminar interface.

2.2. Cement-matrix composites

Cement is a low-cost, mechanically rugged and electrically conducting material which can be rendered n-type or p-type by the use of appropriate admixtures, such as short carbon fibers (which contribute holes) for attaining p-type cement and short steel fibers (which contribute electrons) for attaining n-type cement [16–20]. (Cement itself is weakly n-type in relation to electronic/ionic conduction [16].) The fibers also improve the structural properties, such as increasing the flexural strength and toughness and decreasing the drying shrinkage [21–28]. Furthermore, cement-based junctions can be easily made by pouring the dissimilar cement mixes side by side.

The steel fibers used to provide strongly n-type cement paste were made of stainless steel No. 434, as obtained from International Steel Wool Corp. (Springfield, OH). The fibers were cut into pieces of length 5 mm prior to use in the cement paste in the amount of 0.5% by mass of cement (i.e., 0.10 vol%). The properties of the steel fibers are shown in Table II. The mechanical properties of mortars containing these fibers are described in Ref. 22. However, no aggregate, whether coarse or fine, was used in this work.

The carbon fibers used to provide p-type cement paste were isotropic pitch based, unsized, and of length ~5 mm, as obtained from Ashland Petroleum Co. (Ashland, Kentucky). They were used in the amount of either 0.5% or 0.1% by mass of cement (i.e., either 0.48 or 0.96 vol% in the case of cement paste with silica fume, and either 0.41 or 0.82 vol% in the case of cement paste with latex). Silica fume, due to its fine particulate nature, is particularly effective for enhancing the fiber dispersion [29, 30]. The fiber properties are shown in Table III. No aggregate (fine or coarse) was used. The cement paste with carbon fibers in the amount of 1.0%

by mass of cement was p-type, whereas that with carbon fibers in the amount of 0.5% by mass of cement was slightly n-type, as shown by thermoelectric power measurement [16].

The cement used in all cases was portland cement (Type I) from Lafarge Corp. (Southfield, MI). Silica fume (Elkem Materials, Inc., Pittsburgh, PA, EMS 965) was used in the amount of 15% by mass of cement. The methylcellulose, used in the amount of 0.4% by mass of cement, was Dow Chemical Corp., Midland, MI, Methocel A15-LV. The defoamer (Colloids, Inc., Marietta, GA, 1010) used whenever methylcellulose was used was in the amount of 0.13 vol%. The latex, used in the amount of 20% by mass of cement, was a styrene butadiene copolymer (Dow Chemical Co., Midland, MI, 460NA) with the polymer making up about 48% for the dispersion and with the styrene and butadiene having a mass ratio of 66 : 34. The latex was used along with an antifoaming agent (Dow Corning Corp., Midland, MI, No. 2410, 0.5% by mass of latex).

A rotary mixer with a flat beater was used for mixing. Methylcellulose (if applicable) was dissolved in water and then the defoamer was added and stirred by hand for about 2 min. Latex (if applicable) was mixed with the antifoam by hand for about 1 min. Then the methylcellulose mixture (if applicable), the latex mixture (if applicable), cement, water, silica fume (if applicable), carbon fibers (if applicable) and steel fibers (if applicable) were mixed in the mixer for 5 min.

A junction between any two types of cement mix was made by pouring the two different mixes into a rectangular mold (160 × 40 × 40 mm) separately, such that the time between the two pours was 10–15 min. The two mixes were poured into two side-by-side compartments of the mold and the paper (2 mm thick, without oil on it) separating the compartments was removed immediately after the completion of the two pours. Each compartment was roughly half the length of the entire mold.

After pouring into oiled molds, an external electrical vibrator was used to facilitate compaction and decrease the amount of air bubbles. The resulting junction could be seen visually, due to the color difference between the two halves of a sample. The samples were demolded after 1 day and cured in air at room temperature (relative humidity = 100%) for 28 days.

Five types of cement paste were prepared, namely (i) plain cement paste (weakly n-type, consisting of just cement and water), (ii) steel fiber cement paste (strongly n-type, consisting of cement, water and steel fibers), (iii) carbon-fiber silica-fume cement paste (very weakly n-type, consisting of cement, water, silica fume, methylcellulose, defoamer and carbon fibers in the amount of 0.5% by mass of cement), (iv) carbon-fiber silica-fume cement paste (p-type, consisting of cement, water, silica fume, methylcellulose, defoamer and carbon fibers in the amount of 1.0% by mass of cement), and (v) carbon-fiber latex cement paste (very weakly n-type, consisting of cement, water, latex and carbon fibers). The water/cement ratio was 0.45 for pastes (i), (ii), (iii) and (iv), and was 0.25 for paste (v). The absolute thermoelectric power of each paste is shown in Table IV [16, 20].

TABLE II Properties of steel fibers

Nominal diameter	60 μm
Tensile strength	970 MPa
Tensile modulus	200 GPa
Elongation at break	3.2%
Volume electrical resistivity	$6 \times 10^{-5} \Omega \cdot \text{cm}$
Specific gravity	7.7 g cm^{-3}

TABLE III Properties of carbon fibers

Filament diameter	$15 \pm 3 \mu\text{m}$
Tensile strength	690 MPa
Tensile modulus	48 GPa
Elongation at break	1.4%
Electrical resistivity	$3.0 \times 10^{-3} \Omega \cdot \text{cm}$
Specific gravity	1.6 g cm^{-3}
Carbon content	98 wt.%

TABLE IV Absolute thermoelectric power ($\mu\text{V}/^\circ\text{C}$)

Cement paste	Volume fraction fibers	$\mu\text{V}/^\circ\text{C}$	Type	Ref.
(i) Plain	0	1.99 ± 0.03	Weakly n	[16]
(ii) S_f (0.5*)	0.10%	53.3 ± 4.8	Strongly n	[20]
(iii) C_f (0.5*) + SF	0.48%	0.89 ± 0.09	Weakly n	[16]
(iv) C_f (1.0*) + SF	0.95%	-0.48 ± 0.11	p	[16]
(v) C_f (0.5*) + L	0.41%	1.14 ± 0.05	Weakly n	[16]

Note: SF = silica fume; L = latex.

TABLE V Cement junctions

Junction	Pastes involved	Junction type	Thermocouple sensitivity ($\mu\text{V}/^\circ\text{C}$)	
			Heating	Cooling
(a)	(iv) and (ii)	pn	70 ± 7	70 ± 7
(b)	(iii) and (ii)	nn ⁺	65 ± 5	65 ± 6
(c)	(v) and (ii)	nn ⁺	59 ± 7	58 ± 5

Note. nn⁺ refers to a junction between a weakly n-type material and a strongly n-type material.

Three pairs of cement paste were used to make junctions, as described in Table V. For each pair, three specimens were tested in terms of the thermocouple behavior.

Thermocouple testing was conducted by heating the junction by resistance heating, which was provided by nichrome heating wire (wound around the whole perimeter of the sample over a width of 10 mm that was centered at the junction), a transformer and a temperature controller. The voltage difference between the two ends of a sample was measured by using electrical contacts in the form of copper wire wound around the whole perimeter of the sample at each end of the sample. Silver paint was present between the copper wire and the sample surface under the wire. The copper wires from the two ends were fed to a Keithley 2001 multimeter for voltage measurement. A T-type thermocouple was positioned to almost touch the heating wire at the junction. Another T-type thermocouple was attached to one of the two ends of the sample (at essentially room temperature). The difference in temperature between these two locations governs the voltage. Voltage and temperature measurements were done simultaneously using the multimeter, while the junction temperature was varied through resistance heating. The voltage difference divided by the temperature difference yielded the thermocouple sensitivity.

Fig. 2 show plots of the thermocouple voltage versus the temperature difference (relative to essentially room temperature) for junction (a). The thermocouple voltage increases monotonically and reversibly with increasing temperature difference for all junctions. The thermocouple voltage noise decreases and the thermocouple sensitivity (Table V) and reversibility increase in the order: (c), (b) and (a). The highest thermocouple sensitivity is $70 \pm 7 \mu\text{V}/^\circ\text{C}$, as attained by junction (a) both during heating and cooling. This value approaches that of commercial thermocouples. That junction (a) gives the best thermocouple behavior (in terms of sen-

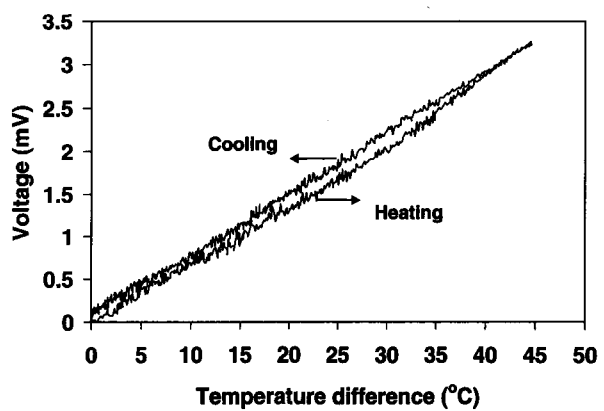


Figure 2 Variation of the cement-based thermocouple voltage with temperature difference during heating and then cooling for junction (a) of Table V.

sitivity, linearity, reversibility and signal-to-noise ratio) is due to the greatest degree of dissimilarity between the materials that make up the junction. The linearity of the plot of thermocouple voltage versus temperature difference is better during cooling than during heating for junction (a).

The values of the thermocouple sensitivity (Table V) are higher than (theoretically equal to) the difference in the absolute thermoelectric power of the corresponding two cement pastes that make up the junction (Table IV). For example, for junction (a), the difference in the absolute thermoelectric power of pastes (iv) and (ii) is $54 \mu\text{V}/^\circ\text{C}$, but the thermocouple sensitivity is $70 \mu\text{V}/^\circ\text{C}$. The reason for this is unclear. Nevertheless, a higher thermocouple sensitivity does correlate with a greater difference in the absolute thermoelectric power.

3. Tailoring by the choice of the interlaminar filler

In contrast to Section 2, which involves dissimilar fibers to make thermocouples from structural composites, this section uses dissimilar interlaminar fillers for the two thermocouple legs, which have identical fibers. Furthermore, in contrast to Section 2.1, which exploits the thermoelectric behavior in the fiber direction of a continuous fiber composite, this section exploits the thermoelectric behavior in the through-thickness direction. The use of dissimilar interlaminar fillers is more suitable for practical application than the use of dissimilar fibers, as the method used to obtain sufficiently dissimilar carbon fibers (i.e., intercalation) is expensive and requires highly crystalline carbon fibers, which are also expensive. Glass fibers and polymer fibers are not suitable, as they are not conducting electrically. Steel fibers are conducting, but their high density makes them unsuitable for lightweight composites. As an interlaminar filler has more effect on the properties (particularly the electrical conduction properties) in the through-thickness direction than those in the fiber direction, this section exploits the thermoelectric behavior in the through-thickness direction.

The thermocouple junction (Section 2.1) that exploits the thermoelectric behavior in the fiber direction involves two dissimilar laminae that form an interlaminar

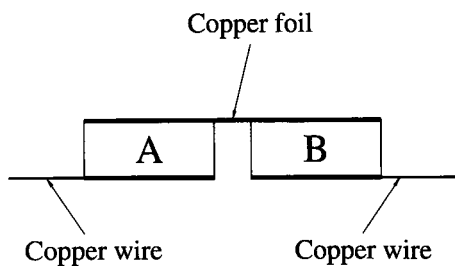


Figure 3 Thermocouple involving dissimilar composites A and B and utilizing the thermoelectric behavior of A and B in the through-thickness direction. In this configuration, the thermocouple junction is exposed.

interface, which is the thermocouple junction. The two laminae can be unidirectional or crossply, but the crossply configuration is attractive in that it provides a two-dimensional array of thermocouple junctions, thereby allowing temperature distribution measurement. Since the thermoelectric behavior in the fiber direction is exploited, only one lamina is needed for each leg. As a consequence, the junction is close to the exposed surface of the laminate and is thus suitable for measuring the temperature of the exposed surface.

On the other hand, for exploiting the thermoelectric behavior in the through-thickness direction, each leg needs to be at least a few laminae in thickness. As a result, the junction is not close to the exposed surface and thus cannot be used to measure the temperature of the exposed surface.

An alternate configuration, as illustrated in Fig. 3, allows the thermocouple junction to be exposed, while each leg comprises multiple laminae. This configuration involves using an electrical interconnection, such as a copper foil that is attached to both laminates. This is the configuration used in this section.

The interlaminar additives used in this section are thermoelectric particles, particularly bismuth, tellurium and bismuth telluride, which are well-known as thermoelectric materials [31].

The thermoplastic polymer was nylon-6 (PA) in the form of unidirectional carbon-fiber (CF) preregs supplied by Quadrax Corp. (Portsmouth, Rhode Island; QNC 4162). The fibers were 34-700 from Grafil, Inc. (Sacramento, California). The fiber diameter was $6.9 \mu\text{m}$. The fiber weight fraction in the prepreg was 62%. The glass transition temperature (T_g) was $40\text{--}60^\circ\text{C}$ and the melting temperature (T_m) was 220°C for the nylon-6 matrix. The prepreg thickness was $250 \mu\text{m}$.

The bismuth particles were from Baker Chemical Co. (Phillipsburg, N.J.). Leico Industries Inc. (New York, N.Y.) supplied the tellurium particles. The bismuth telluride (Bi_2Te_3) particles were supplied by UM Electro-Optic Materials (Hoboken, Belgium). In all cases, the particles had a maximum size of $45 \mu\text{m}$, as obtained by sieving.

Sets 1–5 of composite specimens were obtained as described below. Each specimen was made by stacking eight plies of the prepreg in the unidirectional configuration. For Set 1, no interlaminar filler was used. For Sets 2–5, bismuth, tellurium or bismuth telluride particles respectively were spread out manually on each ply as they were laid up. The composition was the same for

all seven interlayers in the same composite. By using a hydraulic hot press, the stacks obtained were subjected to a pressure of 2 MPa, heated to 260°C at a rate of $5^\circ\text{C}/\text{min}$ and then held at the temperature and pressure for 30 min.

Sets 6–8 of composite specimens were obtained as described below. Each specimen was made by stacking 15 plies of the prepreg in the unidirectional configuration. For Set 6, the 14 interlayers involved alternating layers of tellurium and bismuth telluride particles. For Sets 7 and 8, the composition was the same for all 14 interlayers in the same composite. For Set 7, each interlayer was a mixture of tellurium and bismuth telluride particles (mixed manually before application), such that bismuth telluride particles were in a greater proportion. Set 8 was similar to Set 7, except that tellurium particles were in a greater proportion.

From each of Sets 1–5, two types of specimens were obtained by cutting a laminate. The first type, with a nominal size of $15 \times 12 \text{ mm}$, was used to determine the absolute thermoelectric power in the through-thickness direction. The second type, with a nominal size of $35 \times 6 \text{ mm}$, was used to determine the value in the longitudinal direction. For each of Sets 6–8, only the type for determining the absolute thermoelectric power in the through-thickness direction was obtained by cutting.

To generate a temperature gradient in the through-thickness direction, a specimen of the first type was placed between a hot plate and a cold plate, both lined with an electrically insulating film. For the purpose of voltage measurement, copper wire was laid up on both of the $15 \times 12 \text{ mm}$ surfaces, and then covered with copper foil. A layer of silver paint was applied between the foil and the sample surface. Both, the silver paint and the copper foil helped to enhance the thermal contact.

To obtain a temperature gradient in the longitudinal direction, one of the ends of a specimen of the second type was placed on a hot plate and the other on a cold plate. For voltage measurement, copper wire was wrapped around the perimeter at each end of the specimen and then covered with copper foil, with silver paint between them the foil and the specimen surface.

In both cases the temperature of the hot plate was increased by using a temperature controller, which enabled heating to be conducted at a rate of $0.5^\circ\text{C}/\text{min}$. The temperatures of the hot and cold surfaces of the sample were simultaneously measured by two T-type thermocouples. The voltage difference between them was measured with a Keithley 2001 multimeter. Three specimens of each type were tested.

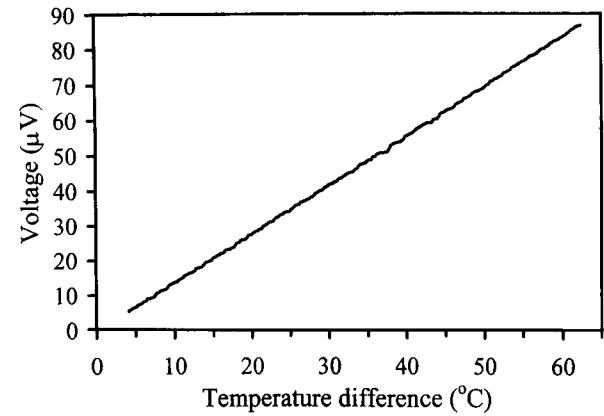
A thermocouple was made using the configuration of Fig. 3. Each of the two dissimilar laminates (A and B in Fig. 3) had eight laminae and an interlaminar additive at each of the seven interlaminar interfaces. One laminate (A) had tellurium particles as the additive; the other laminate (B) had bismuth telluride particles as the additive. The copper foil connecting A and B was attached to A and B by using silver paint, which was applied between the foil and each laminate. For making electrical contact to the ends of A and B away from the copper foil, copper wire, in conjunction with silver paint and a copper foil overlayer, was applied to these ends, as illustrated in Fig. 3.

TABLE VI Density, interlayer particle filler volume fraction and absolute thermoelectric power of various thermoplastic-matrix composites

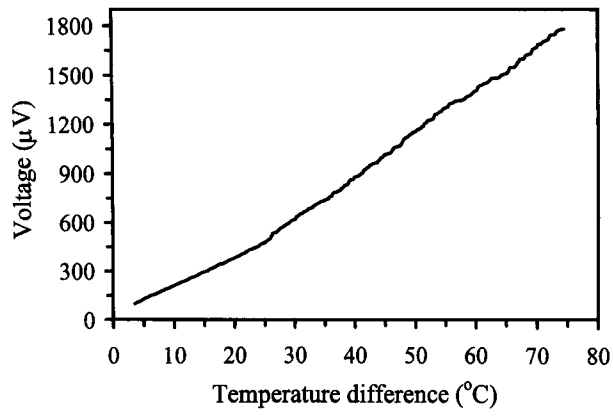
Set	Density (g/cm ³)	Particle filler	Volume fraction particle filler (%)	Absolute thermoelectric power ($\mu\text{V}/^\circ\text{C}$)	
				Through-thickness	Longitudinal
1	1.4 ± 0.2	None	0	+0.5 ± 0.1	-0.7 ± 0.1
2	1.8 ± 0.2	Bi	4.5 ± 0.5	+0.6 ± 0.1	-0.9 ± 0.1
3	2.3 ± 0.2	Bi	10.5 ± 0.5	+1.2 ± 0.1	-0.3 ± 0.1
4	1.8 ± 0.2	Te	7.3 ± 0.5	+22.3 ± 0.2	-0.1 ± 0.1
5	2.1 ± 0.2	Bi ₂ Te ₃	9.9 ± 0.5	-11.7 ± 1.5	-0.8 ± 0.15
6	2.2 ± 0.2	Te	8.0 ± 0.5	+8.2 ± 0.3 ^a	-
		Bi ₂ Te ₃	6.5 ± 0.5	-8.5 ± 1.7 ^b	-
7	2.3 ± 0.2	Te	3.6 ± 0.5	-29.4 ± 2.5	-
		Bi ₂ Te ₃	11.5 ± 0.5	-	-
8	2.3 ± 0.2	Te	14.7 ± 0.5	+53.6 ± 2.5	-
		Bi ₂ Te ₃	3.0 ± 0.5	-	-

^a5–35°C temperature difference.

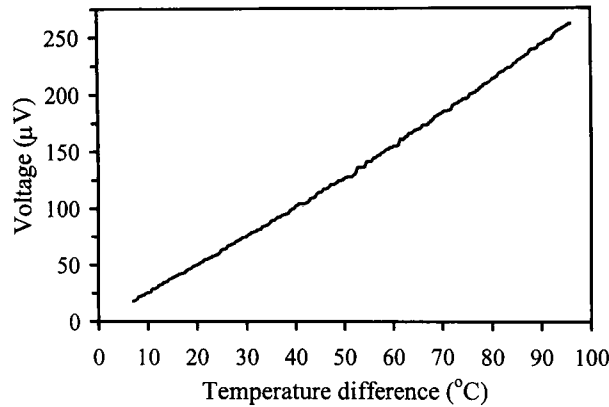
^b55–70°C temperature difference.



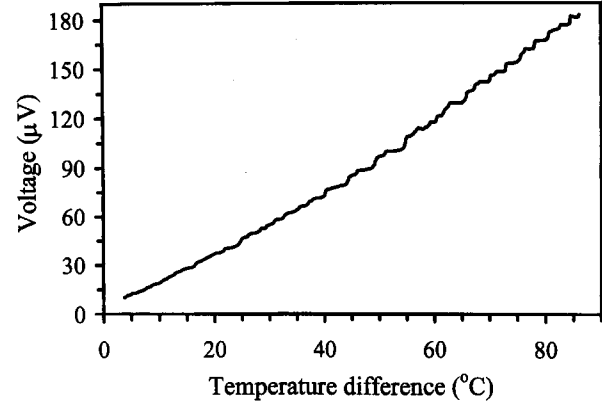
(a)



(a)



(b)



(b)

Figure 4 Seebeck voltage (relative to copper) versus the temperature difference for Set 1 during heating (a) in the through-thickness direction (b) in the longitudinal direction.

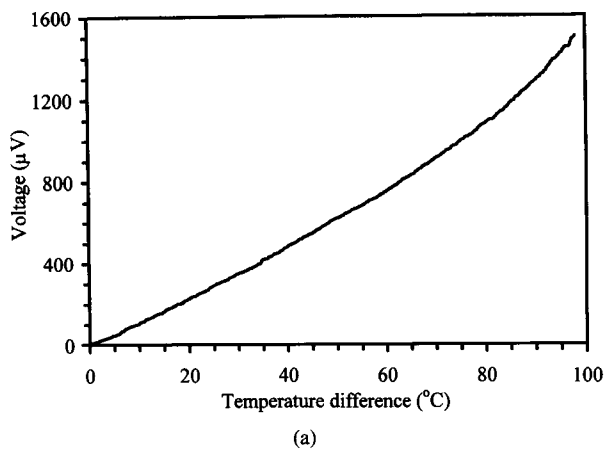
Figure 5 Seebeck voltage (relative to copper) versus the temperature difference for Set 4 during heating (a) in the through-thickness direction (b) in the longitudinal direction.

Figs 4–6 show plots of the measured Seebeck voltage (relative to copper) vs. the temperature difference obtained during heating for Sets 1, 4 and 5 respectively. In all the cases, the data points fall on a nearly straight line through the origin, and the curves for heating and cooling are similar. Table VI shows the absolute thermoelectric power obtained in the through-thickness and longitudinal directions for the composites investigated.

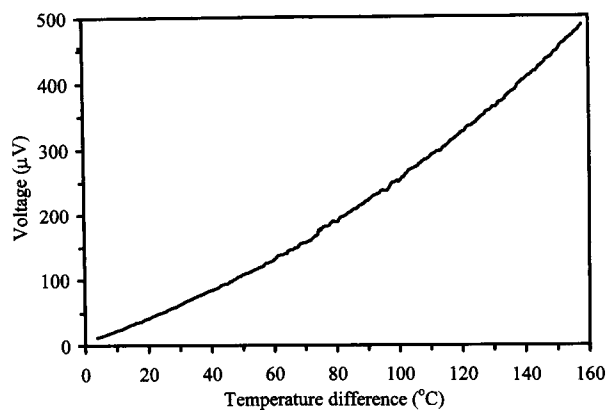
As can be seen, even though the sign of the absolute thermoelectric power is different in the directions considered, the addition of the interlaminar thermoelectric particles tends to make it more positive in most cases.

The effect is larger in the through-thickness direction than in the longitudinal direction. The thermoelectric behavior of the composite material is influenced by the reinforcing fibers and the interlaminar interfaces. While the fibers govern the behavior in the longitudinal direction, the interlaminar interfaces are encountered in the through-thickness direction. As a result, the effect of the interlaminar particles on the thermal or electrical conduction is expected to be larger in the through-thickness direction than in the longitudinal direction.

The use of tellurium particles is more effective than the use of bismuth particles in making the absolute



(a)



(b)

Figure 6 Seebeck voltage (relative to copper) versus the temperature difference for Set 5 during heating (a) in the through-thickness direction (b) in the longitudinal direction.

thermoelectric power more positive, particularly in the through-thickness direction. This is because in this direction the sign of the absolute thermoelectric power is the same (positive) for the carbon fiber polymer-matrix composite without interlayer and for tellurium ($+70 \mu\text{V}/^\circ\text{C}$ [31]), and this is a favorable condition for the enhancement of the thermoelectric effect in composite thermoelectrics [32].

In contrast to bismuth ($-72 \mu\text{V}/^\circ\text{C}$ [31]) and tellurium ($+70 \mu\text{V}/^\circ\text{C}$ [31]), bismuth telluride ($+200 \mu\text{V}/^\circ\text{C}$ [31]) makes the absolute thermoelectric power of the composite more negative, particularly in the through-thickness direction. The origin of this effect is unclear.

Because tellurium and bismuth telluride as interlaminar fillers give opposite signs of the absolute thermoelectric power, they were used for making a composite thermocouple using the configuration of Fig. 3. Fig. 7 shows that the curve of the thermocouple voltage vs. temperature difference is linear. The thermoelectric sensitivity (e.g., thermocouple voltage per unit temperature difference) is $30 \pm 1.5 \mu\text{V}/^\circ\text{C}$, which, as expected, is roughly equal to the sum of the magnitudes of the absolute thermoelectric power of the two legs in the through-thickness direction (Table VI).

Figs 8–10 show plots of the measured Seebeck voltage (relative to copper) vs. the temperature difference obtained during heating for Sets 6–8 respectively. In Fig. 8, the slope of the curve changed reversibly in sign as the temperature difference increased. In the temper-

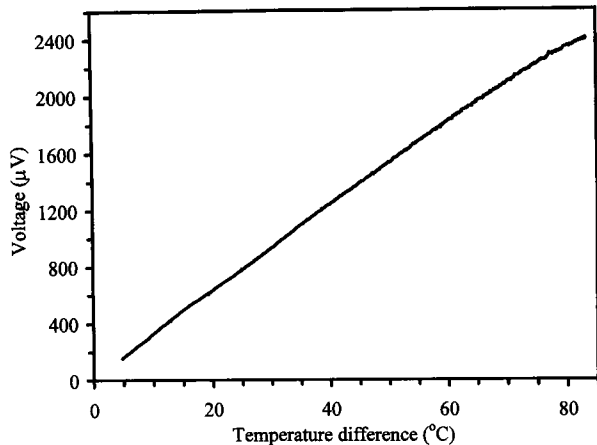


Figure 7 Thermocouple voltage vs. temperature difference for a thermocouple with the configuration of Fig. 3 and involving as the two legs of the thermocouple a Set 4 composite and a Set 5 composite.

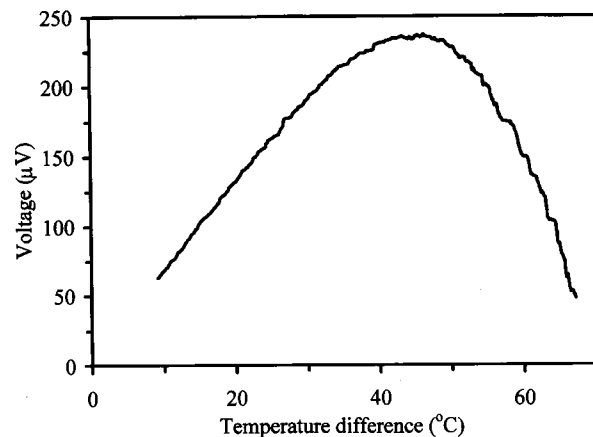


Figure 8 Seebeck voltage (relative to copper) versus the temperature difference for Set 6 during heating in the through-thickness direction.

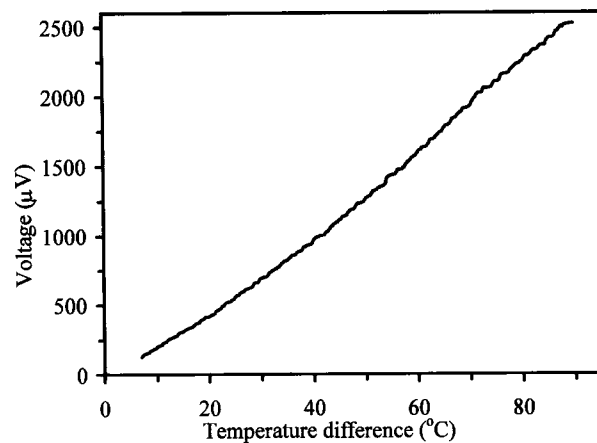


Figure 9 Seebeck voltage (relative to copper) versus the temperature difference for Set 7 during heating in the through-thickness direction.

ature difference range of $5\text{--}35^\circ\text{C}$, the absolute thermoelectric power in the through-thickness direction was $+8.2 \pm 0.3 \mu\text{V}/^\circ\text{C}$; in the temperature difference range of $55\text{--}70^\circ\text{C}$, the value was $-8.5 \pm 1.7 \mu\text{V}/^\circ\text{C}$. In Figs 9 and 10, there was no change in sign of the slope within a plot, though the slope increased slightly when the temperature difference was high in Fig. 9 and the slope decreased slightly when the temperature difference was high in Fig. 10.

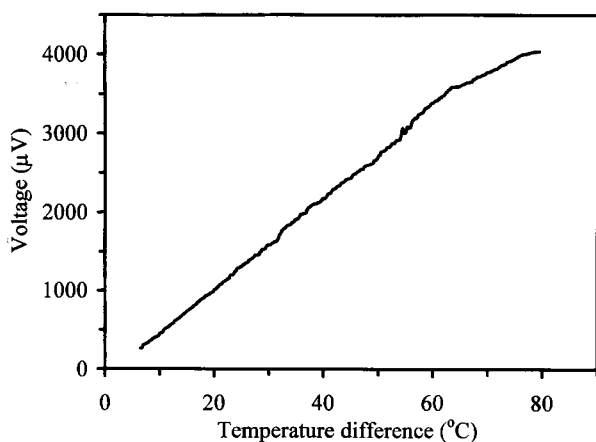


Figure 10 Seebeck voltage (relative to copper) versus the temperature difference for Set 8 during heating in the through-thickness direction.

Of significance is that the absolute thermoelectric power is strongly negative ($-29.4 \pm 2.5 \mu\text{V}/^\circ\text{C}$) for Fig. 9 (the case in which bismuth telluride dominated) and is strongly positive ($+53.6 \pm 2.5 \mu\text{V}/^\circ\text{C}$) for Fig. 10 (the case in which tellurium dominated). That the case in which bismuth telluride dominated (Set 7) gave a negative value of the absolute thermoelectric power is consistent with the negative value for the case in which bismuth telluride was the sole interlayer filler (Set 5), but the presence of a small proportion of tellurium along with bismuth telluride caused the absolute thermoelectric power to become much more negative. That the case in which tellurium dominated (Set 8) gave a positive value of the absolute thermoelectric power is consistent with the positive value for the case in which tellurium was the sole interlayer filler (Set 4), but the presence of a small proportion of bismuth telluride along with tellurium caused the absolute thermoelectric power to become much more positive.

The origin of the change in sign of the slope in Fig. 8 is unclear, but it may relate to the dominating effect of bismuth telluride in the high range of temperature difference (so that the absolute thermoelectric power is negative) and the dominating effect of tellurium in the low range of temperature difference (so that the absolute thermoelectric power is positive). The increase in slope when the temperature difference is large in Fig. 9 and the decrease in slope when the temperature difference is large in Fig. 10 may have origins that are similar to that of the change in sign of the slope in Fig. 8.

In Set 6, the proportions of tellurium and bismuth telluride were comparable, even though these fillers were not mixed in the same interlayer. The values of the absolute thermoelectric power ($+8.2$ and $-8.5 \mu\text{V}/^\circ\text{C}$, depending on the temperature difference) for Set 6 are intermediate between those for Set 7 (bismuth telluride dominating, $-29.4 \mu\text{V}/^\circ\text{C}$) and Set 8 (tellurium dominating, $+53.6 \mu\text{V}/^\circ\text{C}$). Although the case of tellurium and bismuth telluride in comparable proportions and mixed in each interlayer was not investigated, it is likely that this case will give similar results as Set 6.

By using a combination of two thermoelectric materials (combination of Sets 4 and 5 in the through-thickness direction) that exhibit opposite signs of the absolute thermoelectric power, such that one material

(i.e., one filler in the interlayer) dominated over the other (Sets 7 and 8), we attained magnitudes of the absolute thermoelectric power that are much higher than those of the corresponding materials by themselves (i.e., with only one type of thermoelectric filler in the interlayer). This behavior has not been previously reported, but it is consistent with related prior work on composite thermoelectrics [32,33].

Tellurium (as an element) has an absolute thermoelectric power of $+70 \mu\text{V}/^\circ\text{C}$ [31]. By having just 7.3 vol% Te in a carbon fiber polymer-matrix composite (Set 4), an absolute thermoelectric power of $+22 \mu\text{V}/^\circ\text{C}$ (31% of the value of tellurium as an element) was attained in the through-thickness direction. Even though the carbon fiber polymer-matrix composite without an interlayer (Set 1) is negligibly small in its absolute thermoelectric power ($+0.5 \mu\text{V}/^\circ\text{C}$), its presence along with a small proportion of tellurium has a synergistic effect that results in an unexpectedly high value of the absolute thermoelectric power in the through-thickness direction. The origin of this synergistic effect is presently not clear, but the effect is consistent with the previous report of enhancement of the absolute thermoelectric power by combination of a "high quality thermoelectric" and a "benign metal" [32].

Set 8 gave a high value of the absolute thermoelectric power, i.e., $+54 \mu\text{V}/^\circ\text{C}$. This high value is of technological importance.

4. Conclusion

The tailoring of the thermoelectric properties (the sign and magnitude of the absolute thermoelectric power) was achieved by composite engineering. The techniques involved the choice of the reinforcing fibers (continuous or short) in a structural composite and the choice of the filler between the laminae in a continuous fiber composite. The tailoring resulted in thermoelectric structural composites, including continuous carbon fiber polymer-matrix composites and short fiber cement-matrix composites. In addition, it resulted in thermocouples in the form of structural composites. The choice of fibers impacted the thermoelectric behavior in the fiber direction of the composite. The choice of interlaminar filler impacted the thermoelectric behavior in the through-thickness direction.

The choice of fibers encompassed that between p-type fibers (e.g., pristine and acceptor-intercalated carbon fibers) and n-type fibers (e.g., donor-intercalated carbon fibers and steel fibers). In case of continuous fibers, a thermocouple resulted from the use of dissimilar fibers, such that the thermocouple junction was the interface between polymer-matrix laminae of dissimilar fibers. In case of short fibers, a thermocouple junction was provided by a cementitious bond between cement-matrix composites containing dissimilar fibers.

Interlaminar fillers between continuous carbon fiber polymer-matrix laminae were thermoelectric particulate fillers such as tellurium and bismuth telluride. The use of a mixture of dissimilar fillers, such that one filler dominated over the other, resulted in enhancement of the through-thickness Seebeck effect over that for the case of a single filler (the dominating one) being used.

With tellurium dominating over bismuth telluride, an absolute thermoelectric power of $+54 \mu\text{V}/^\circ\text{C}$ was attained, compared to the value of $+22 \mu\text{V}/^\circ\text{C}$ when tellurium alone was used. With bismuth telluride dominating over tellurium, an absolute thermoelectric power of $-29 \mu\text{V}/^\circ\text{C}$ was attained, compared to a value of $-12 \mu\text{V}/^\circ\text{C}$ when bismuth telluride alone was used.

The use of dissimilar interlaminar fillers resulted in dissimilar composites, the junction of which served as a thermocouple junction. In this work, the junction was obtained by electrically connecting the top laminae of two dissimilar laminates.

References

1. M. S. DRESSELHAUS, *Materials Science & Engineering B—Solid State Materials for Advanced Technology* **3/4** (1988) 259.
2. S. FLANDROIS, C. HAUW and R. B. MATHUR, *Synthetic Metals* **34**(1–3) (1989/1990) 399.
3. K. LUEDERS and R. SCHOELLHORN (ed.), *ibid.* **34**(1–3) (1989/1990) p. 762.
4. J. TSUKAMOTO, A. TAKAHASHI, J. TANI and T. ISHIGURO, *Carbon* **27**(6) (1989) 919.
5. C. T. HO and D. D. L. CHUNG, *ibid.* **28**(6) (1990) 825.
6. V. GUPTA, R. B. MATHUR, O. P. BAHL, A. MARCHAND and S. FLANDROIS, *ibid.* **33**(11) (1995) 1633.
7. D. E. WESSBECHER, W. C. FORSMAN and J. R. GAIER, *Synth. Met.* **26**(2) (1988) 185.
8. C. HÉROLD, A. HÉROLD and P. LAGRANGE, *J. Phys. Chem. Solids* **57**(6–8) (1996) 655.
9. J. R. GAIER, P. D. HAMBOURGER and M. E. SLABE, *Carbon* **29**(3) (1991) 313.
10. J. R. GAIER, M. L. DAVIDSON and R. K. SHIVELY, in *Technology Transfer in a Global Community*, Int. SAMPE Tech. Conf., 1996 (SAMPE, Covina, CA, 1996) Vol. 28, p. 1136.
11. M. KATSUMATA, M. ENDO, H. YAMANASHI and H. USHIJIMA, *J. Mater. Res.* **9**(7) (1994) 1829.

12. D. D. L. CHUNG, in "Carbon Fiber Composites" (Butterworth-Heinemann, 1994).
13. C. T. HO and D. D. L. CHUNG, *Carbon* **28**(6) (1990) 831.
14. D. D. POLLOCK, in "Thermoelectricity: Theory, Thermometry, Tool," ASTM Special Technical Publication 852 (ASTM, Philadelphia, PA, 1985) p. 121.
15. S. WANG and D. D. L. CHUNG, *Compos. Interfaces* **6**(6) (1999) 497.
16. S. WEN and D. D. L. CHUNG, *Cem. Concr. Res.* **29**(12) (1999) 1989.
17. M. SUN, Z. LI, Q. MAO and D. SHEN, *ibid.* **28**(4) (1998) 549.
18. *Idem.*, *ibid.* **28**(12) (1998) 1707.
19. *Idem.*, *ibid.* **29**(5) (1999) 769.
20. S. WEN and D. D. L. CHUNG, *ibid.* **30**(4) (2000) 661.
21. P.-W. CHEN and D. D. L. CHUNG, *Composites B* **27B** (1996) 269.
22. *Idem.*, *ACI Mater. J.* **93**(2) (1996) 129.
23. A. M. BRANDT and L. KUCHARSKA, in *Materials for the New Millennium*, Proc. Mater. Eng. Conf., 1996 (ASCE, New York, NY, 1996) Vol. 1, p. 271.
24. N. BANTHIA and J. SHENG, *Cem. Concr. Compos.* **18**(4) (1996) 251.
25. B. MOBASHER and C. Y. LI, *ACI Mater. J.* **93**(3) (1996) 284.
26. M. PIGEON, M. AZZABI and R. PLEAU, *Cem. Concr. Res.* **26**(8) (1996) 1163.
27. N. BANTHIA, C. YAN and K. SAKAI, *ibid.* **20**(5) (1998) 393.
28. T. URANO, K. MURAKAMI, Y. MITSUI and H. SAKAI, *Composites A: Applied Science & Manufacturing* **27**(3) (1996) 183.
29. P.-W. CHEN and D. D. L. CHUNG, *J. Electron. Mater.* **24**(1) (1995) 47.
30. P.-W. CHEN, X. FU and D. D. L. CHUNG, *ACI Mater. J.* **94**(3) (1997) 203.
31. R. A. HORNE, *J. Appl. Phys.* **30** (1959) 393.
32. D. J. BERGMAN and L. G. FEL, *ibid.* **85**(12) (1999) 8205.
33. D. J. BERGMAN and O. LEVY, *ibid.* **70**(11) (1991) 6821.

Received 13 November 2001
and accepted 3 June 2002